

PERFORMANCE DETERIORATION AND MICROSTRUCTURE OF VITRIFIED MICROBEAD INSULATION CONCRETE AFTER HIGH TEMPERATURE

Leandro T. Azevedo
State University of the Northern Rio de Janeiro, Brazil.

Abstract: Prepare ordinary concrete (NC) and vitrified microbead insulation concrete (GHB/NC), and study the deterioration process of changes in apparent phenomena, quality, loss of compressive strength and other properties after heating from normal temperature to 1000°C, and discuss ultrasonic non-destructive testing at the same time. The method is used to evaluate the universality of the performance of concrete after high temperatures, comparatively analyze the relationship between relative wave speed, damage degree, heating temperature, and compressive strength loss rate, and use SEM to observe the microstructural changes of specimens after different high temperatures.

The results show that the use of relative wave speed and damage degree to evaluate the performance of concrete after high temperature has good correlation, and the regression formula has a high fitting degree; as the temperature increases, the internal damage of NC and GHB/NC concrete gradually intensifies, and the cement gelation decomposes due to heat and moisture Dissipation, etc. produce gaps, cracks and interconnections on the surface and inside of the specimen, and the bonding force at the interface between vitrified microspheres, coarse aggregate and cement stone gradually weakens or even loses, causing the macroscopic mechanical properties to deteriorate and the compressive strength loss rate to increase. After heating to 800°C, the strength loss of NC is 72.3%, the strength loss of GHB/NC is 74.6%, and the load-bearing capacity is basically lost at 1000°C.

Keywords: Vitrified microbead insulation concrete; High temperature; Ultrasonic nondestructive testing; Performance degradation; Microscopic analysis; Interface transition zone

1 EXPERIMENTAL MATERIALS AND METHODS

At present, my country's building energy consumption accounts for a large proportion of national energy consumption and is on the rise. Therefore, building energy conservation is a topic of widespread concern at present. The key is to improve the heat insulation and heat preservation performance of the building envelope to reduce indoor heat loss and save energy [1]. Commonly used external wall insulation systems include insulation systems based on organic insulation materials such as polystyrene particles and polystyrene boards, and insulation systems based on inorganic insulation materials such as vitrified microbead insulation mortar and expanded vermiculite insulation mortar [2- 3]. A large number of engineering practices have proven that organic materials have poor durability and fire resistance, while inorganic materials have excellent properties such as heat insulation, fire retardancy, high temperature resistance, and green environmental protection, and have gradually received widespread attention and application [4].

Research on vitrified microbead inorganic exterior wall insulation materials focuses on the discussion of the performance of thermal insulation mortar. For example, Gong Jianqing et al. [5] studied the effect of different water-binder ratios on the performance of vitrified microbead thermal insulation mortar; Zhu Jiang et al. [6] discussed the influence of propylene fiber content on the mechanical properties and softening coefficient of vitrified microsphere composite insulation materials; Wu Wenjie et al. [7] analyzed the influence of each component of thermal insulation mortar on material properties. However, using insulation mortar as exterior wall insulation material increases the construction process. Therefore, relevant scholars have proposed vitrified microsphere insulation concrete materials that can effectively bear load and have thermal insulation functions. MA et al. [8], ZHAO et al. [9], ZHANG [10] and Dai Xueling et al. [11] conducted a series of studies on this, including the macroscopic physical and mechanical properties, thermal insulation capabilities, microscopic characteristics, etc. of the material, as well as the exploration and application of structural self-insulating walls. practice. However, there are few studies on vitrified microbead self-insulating concrete after high-temperature fires. The use of ultrasonic non-destructive testing to evaluate the internal damage of building structures is a convenient, fast, and highly repeatable method [12]. Since vitrified microbeads The beads are mixed into cement mortar as fine aggregate so that the bonding with the cement stone is different from that of conventional concrete, and the ultrasonic wave propagation characteristics are also different. However, there are few public reports on the use of ultrasonic method to evaluate the performance of vitrified microbead concrete after high temperature. Relevant studies have shown that cement slurry becomes more loose and porous after high temperature, causing the occurrence and development of macro cracks [13-14]. However, the unique embedded interface structure of vitrified microspheres and cement stones is different from ordinary concrete [15]. Structural changes in the interface zone and internal degradation processes and mechanisms after high temperatures deserve attention.

To this end, this article tests the quality and strength loss of vitrified microsphere thermal insulation concrete (GHB/NC) after high temperature treatment. Non-destructive ultrasonic detection technology is used to use relative wave speed and

damage degree as evaluation indicators to analyze the interior of the material after different temperatures. Damage and strength loss rate, use scanning electron microscope to observe the microstructural changes of the specimen after high temperature. Exploring the high-temperature degradation mechanism of vitrified microbead insulation concrete from macro and micro perspectives.

1.1 Raw Materials

The cement uses Huainan Bagongshan brand P·C42.5 grade composite Portland cement. Its 3-day and 28-day compressive strengths are 29.99 MPa and 49.75 MPa respectively. Huainan Pingwei Power Plant produces grade I fly ash., its chemical composition content is shown in Table 1; the fine aggregate is medium sand, with a fineness modulus of 2.8; vitrified microbeads produced by Henan Xinyang Jinhualan Company are used as lightweight fine aggregate, and its main performance indicators are shown in Table 2 ; The coarse aggregate is calcareous gravel with a particle size of 5 to 15 mm and is continuously graded; the admixture is HPWR high-performance water-reducing agent produced by Shaanxi Qinfen Building Materials.

Vitrified microbeads (GHB) are a kind of non-metallic lightweight thermal insulation material. They are formed by crushing, screening and vitrification of turpentine ore after mining, instantaneous combustion at high temperature, and vitrification. They are porous inside and vitrified on the surface, and are in the form of spherical fine particles. diameter particles. The micromorphology of vitrified microbeads observed using scanning electron microscopy (SEM) is shown in Figure 1. It can be seen that the interior has a honeycomb porous structure. This special structure extends the heat transfer path inside the material and increases the internal pores, allowing heat to spread both in the material and in the air, and the air itself is a good thermal insulation material., the thermal conductivity is only 0.023W/(m·K)[16], thereby increasing energy dissipation loss and improving thermal insulation capacity; while the outer surface is vitrified and closed in a spherical shape, but it is easily squeezed during the concrete mixing process. Broken due to pressure, vibration, etc., resulting in loss of strength.

1.2 Concrete Mix Proportion Design

According to JGJ55 - 2011 [17], the concrete mix ratio was designed. The vitrified microspheres were subjected to water absorption treatment for 1 hour before the experiment. After the experimental trial mix, the water-cement ratio was adjusted accordingly to ensure consistent water consumption. The specific data are shown in Table 3, where NC (Normal concrete) is C30 ordinary concrete, and GHB/NC (Glazed hollow bead insulation normal concrete) is vitrified microbead insulation concrete. The basic performance test results are shown in Table 4. It can be seen that after adding vitrified microsphere lightweight aggregate, the apparent density, compressive strength, and thermal conductivity of concrete are reduced to varying degrees. The compressive strength at 28 days decreased by about 29%, and the thermal conductivity decreased by about 26 %. Due to the good water retention of vitrified microspheres, the moisture content has increased. After pre-wet treatment, the workability and fluidity of the mixture are greatly improved, which is in line with the current multi-functional requirements of building materials such as lightweight, good workability, and thermal insulation development trend.

Table 1 Chemical composition of fly ash (wt%)

Composition	SiO ₂	Al ₂ O ₃	Fe ₂ O ₃	CaO	MgO	Na ₂ O	Lgnitionloss
Content	53.26	34.72	4.07	2.47	0.39	1.9	4.07

Table 2 Performance indicators of vitrified microspheres

Particle size/mm	Bulk density/ (kg·m ⁻³)	Apparent density/ (kg·m ⁻³)	density/Cylinder strength/MPa	compressive strength/MPa	Thermal conductivity/ (W·(m·K) - 1)	(R efractoriness/°C	Volumeloss rate at 1 MPa/%
0.5-1.5	80-120	80-130	≥150		0.032-0.045	1280-1360	38-46

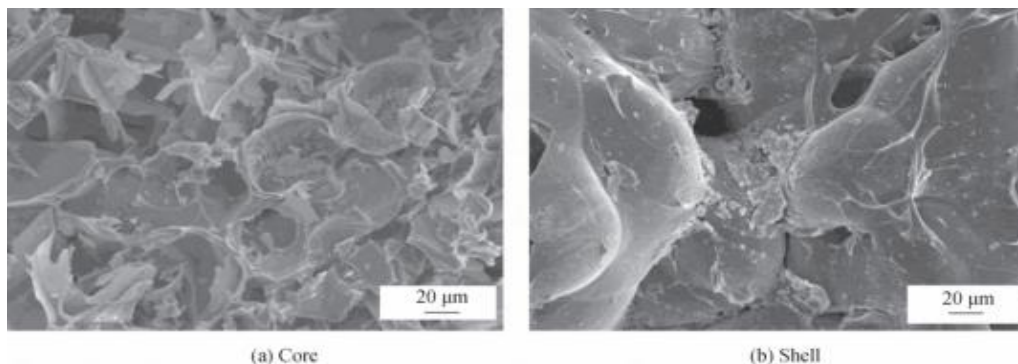


Figure 1 Microstructure morphology of vitrified microbeads (GHB)

Table 3 Concrete mix ratio (kg/m³)

Concrete	Cementing material		Gravel	Fine aggregate		Water	Water reducer	Water cement ratio
	Cement	Flyash		Sand	Glazed hollow bead			
NC	421	47	856	856	—	177.84	4.68	1 : 0.38
GHB/NC	421	47	856	571	100	168.48	4.68	1 : 0.36

Notes: NC— Normal concrete; GHB/NC— Glazed hollow bead insulation normal concrete.

Table 4 Basic performance of mixed soil

Concrete	Workability		Compressive strength/MPa		28d apparent density/(kg·m ⁻³)	28d moisture content/%	Thermal conductivity/(W·(m·K) ⁻¹)
	Slump/mm	Slump flow/mm	3D	28d			
NC	175	350	15.61	36.80	2 272	1. 10	1. 65
GHB/NC	200	410	8.12	26.13	2 102	1. 73	1. twenty two

1.3 Experimental Methods

A cube test block with a size of 100 mm × 100 mm × 100 mm is used. The mold is removed after 1 day of molding and cured under standard curing conditions (relative humidity ≥ 95%, temperature (20 ± 1) °C) for 28 days. Before the experiment, all test blocks were placed in an oven at (105±5) °C to dry for 24 hours to eliminate the influence of moisture in the test blocks on the experiment. A box-type resistance furnace is used to heat the test block. The design target temperature is 100~1000°C, the temperature interval is 100°C, and the heating rate is 10~15°C/min. After rising to the target temperature, the temperature is kept constant for 2 hours to ensure that the furnace temperature and the internal temperature of the test piece are maintained. Consistent, cool the furnace to about 100°C, take out the furnace and let it stand for more than 48 hours to measure various properties of the specimen.

The NM-4B non-metal ultrasonic detector produced by Beijing Kangkerui Company was used to measure the sound speed, main frequency and amplitude of the specimen at each temperature. Each specimen was arranged with 2 relative measuring points to calculate the average. The ultrasonic frequency was 50kHz and the emission was set. The voltage was 500 V and the sampling period was 0. 4 μs; after ultrasonic measurement, the CSS-YAN3000 press produced by Changchun Testing Machine Research Institute was used to conduct a pressure failure experiment. According to the difference between the compressive strength of each specimen after high temperature and drying treatment ratio, and calculate the strength loss rate; finally, samples were taken from the crushed test blocks, and a Hitachi S-3400N scanning electron microscope was used to select the connecting parts of cement stone, vitrified microspheres and cement stone for microscopic morphology observation of the interface area.

2 RESULTS AND DISCUSSION

2.1 Appearance Phenomenon of Concrete at High Temperature

It was observed that the appearance phenomena of NC and GHB/NC concrete specimens after high temperature are similar, as shown in Table 5. It can be seen that as the temperature increases, the appearance color gradually deepens from blue-gray and then lightens to off-white to white. When the temperature is lower than 300°C, there is no obvious change in the appearance of the specimen, the knocking sound is crisp and no cracks occur; when 300~500°C, the color of the specimen deepens and is slightly brown, the knocking sound becomes gentler, and fewer fine cracks appear. The reason is that the coarse aggregate itself does not change significantly in this temperature range, and the cracks and deformation are mainly concentrated in the coarse aggregate and cement. Fine cracks appear at the interface of the mortar matrix and inside the cement mortar matrix. In addition, the calcium ferrite hydrate in the concrete reacts with Ca (OH) 2 to generate brown Fe(OH) 3 precipitation, causing the specimen to appear slightly brown [18].

Table 5 Appearance phenomena of NC and GHB/NC concrete specimens at various temperatures

Temperature/°C	Apparent color of specimen	Knocking sound of specimen	Crack, scaling and loose
20	Cineros	Clear and melodious	None
100	Cineros	Clear and melodious	None
200	Cineros	Slightly clear and melodious	None
300	Slightly brown	Slightly clear and melodious	None
400	Medium brown	Gentle	Minor crack
500	Brown	Gentle	Minor crack
600	Grey white	Slightly low	Obvious crack
700	Grey white	Slightly low	Obviously crack, mild loose
800	White	Low	Obviously crack, a small number of long and wide cracks, increasing loose
900	White	Low	Coarse crack, peeling and scaling, obviously loose
1 000	White	Low	Coarse and through cracks, broken, missing corners, looseness

When the temperature is higher than 600°C, obvious cracks will appear, the appearance will be off-white, and the knocking sound will be low; when the temperature is 800°C, the specimen will turn white, and long cracks will appear; when the temperature exceeds 900°C, a large amount of peeling and peeling will occur. Leave it for 48 hours. The phenomenon of broken and missing corners is serious, the overall structure is loose, and the strength is seriously reduced. The reasons are that the limestone gravel decomposes into CO₂ after being decomposed into CO₂ at a high temperature of 600°C, the volume expansion of cement mortar and other materials after high temperature, and the different thermal expansion coefficients of the gravel and cement mortar matrix. The cracks in the specimen increase and the strength is lost [19-20].

2.2 Quality Loss of Raw Materials and Concrete at High Temperatures

Figure 2 shows the mass loss of each main raw material and concrete specimen with temperature changes. The quality of gravel remains basically unchanged when the temperature is lower than 600°C. The mass loss is about 5% at 600~800°C. The quality drops significantly at 900°C. The mass loss reaches 40% at 1000°C. Sand experiences high temperatures. The final quality loss is small. Since the main component of gravel is CaCO₃, it decomposes into CaO and CO₂ at a temperature of 600~820°C, resulting in significant quality reduction [21].

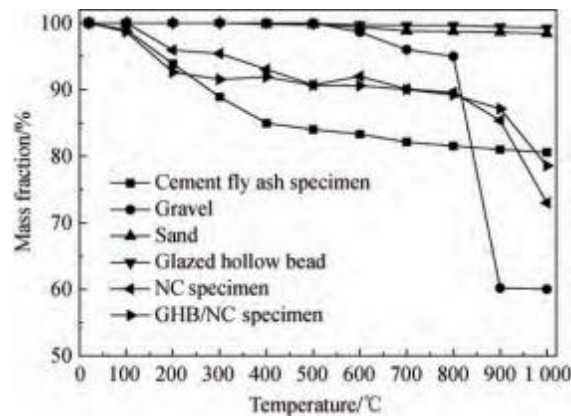


Figure 2 Quality loss of raw materials and concrete after high temperature

After experiencing a high temperature of 1,000°C, the mass loss rate of vitrified microspheres is less than 1%, and the strength and quality are almost unaffected. This is because the vitrified microspheres are processed by a special expansion and firing method. The temperature exceeds 1000°C. Comparing the appearance characteristics of gravel and vitrified microspheres after high temperature treatment at 1000°C (Figure 3), it can be seen that the gravel has changed from bluish white to snow white, with a large loss of strength, while the vitrified microspheres have changed from White particles have no obvious change when heated to 700°C. When the temperature continues to rise to 1000°C, they gradually turn into red particles with a small amount of agglomeration. Figure 4 shows the microstructure of vitrified microbeads after high temperature at 1000°C, and the micromorphology at normal temperature. (Figure 1) Comparison, there is almost no change between the two, indicating that the material is an excellent high temperature resistant material.



Figure 3 Appearance changes of gravel and vitrified microspheres after high temperature

The mass loss trend of the two groups of specimens after experiencing high temperatures is consistent. When the temperature is lower than 200°C, the mass loss is less than 5%. When the temperature is lower than 600°C, the mass loss is controlled at 10%. At this time, the mass loss is mainly caused by the mass loss of cement gel. As a result, the quality further decreases when the temperature exceeds 600°C, and the quality decreases significantly when the temperature reaches 800°C. The mass loss of NC specimens after high temperature treatment at 1000°C reaches 27.01%. After GHB/NC treatment at 1000°C, the quality loss is 21.44%, which is better than NC, reflecting the advantages of vitrified microsphere lightweight aggregate in high temperature resistance compared with sand and gravel.

2.3 High-Temperature Internal Damage to Concrete

Ultrasonic testing is used to evaluate the internal damage of the test block after high temperature treatment. The ultrasonic propagation characteristics are affected by the type, particle size, cement type and dosage of coarse and fine aggregates. Referring to the literature [12], the relative wave speed, damage degree, relative main frequency and The relative amplitude is calculated as the evaluation parameter as follows:

$$vR = vT / v0 \quad (1)$$

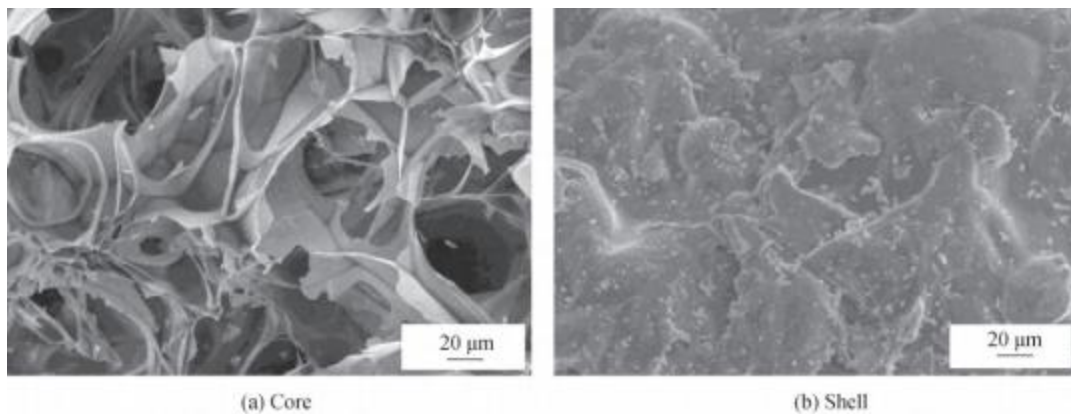


Figure 4 Microstructural morphology of vitrified microbeads after high temperature of 1000°C

Table 6 Processing of concrete ultrasonic test results

Group	Temperature/°C	Relative v	Damage Degree D	Relative dominant frequency fR	Relative amplitude AR	Compressive strength loss rate/%
NC	100	0.976	0.047	0.997	1.599	-6.5
	200	0.886	0.215	0.997	1.545	-11.2
	300	0.773	0.403	1.029	1.639	-20.5
	400	0.641	0.589	1.019	1.537	-24.5
	500	0.539	0.709	0.951	1.662	12.7
	600	0.375	0.859	1.006	1.649	26.2
	700	0.295	0.913	0.987	1.518	38.6
	800	0.277	0.923	0.985	1.342	72.3
	900	0.209	0.956	0.377	0.932	79.0
	1000	0.176	0.969	0.219	0.756	88.5
GHB/NC	100	0.970	0.059	1.009	0.996	-2.7
	200	0.811	0.343	1.019	1.103	-20.6
	300	0.599	0.641	0.975	1.086	-14.8
	400	0.510	0.740	0.990	1.084	-2.1
	500	0.367	0.865	0.997	1.038	20.5
	600	0.324	0.895	1.004	1.062	21.7
	700	0.302	0.909	0.968	0.926	57.7
	800	0.234	0.945	0.519	0.707	74.6
	900	0.185	0.966	0.087	0.660	85.8
	1000	0.127	0.984	0.104	0.486	88.2

Note: Negative value in the compressive strength loss rate indicates an increase in strength at the target temperature.

$$D = 1 - (vT / v0)^2 \quad (2)$$

$$AR = AT / A0 \quad (3)$$

$$fR = fT / f0 \quad (4)$$

$$\Delta Fcu = 1 - FcuT / Fcu0 \quad (5)$$

In the formula: vR is the relative wave speed; vT is the wave speed after high temperature of the specimen (m/s); $v0$ is the wave speed of the specimen before high temperature (m/s); D is the damage degree of the specimen; AR is the relative amplitude; AT is the first wave amplitude after high temperature (dB); $A0$ is the first wave amplitude before high temperature value (dB); fR is the relative dominant frequency; fT is the dominant frequency of the first wave after high temperature (kHz); $f0$ is the dominant frequency of the first wave before high temperature (kHz); ΔFcu is the compressive strength loss rate; $FcuT$ is the resistance of the specimen after high temperature damage Compressive strength value (MPa); $Fcu0$ is the compressive strength value (MPa) of the specimen before high temperature treatment. The measured raw data were processed, and the results are shown in Table 6. It can be seen that the relative amplitude and relative main frequency do not change much when the heating temperature is lower than 800°C. After experiencing high temperatures above 800°C, the amplitude and main frequency decrease significantly, indicating that these two

parameters are very important for evaluating the specimen. The reflection of internal property differences of heated materials is insensitive and is not suitable as an evaluation parameter.

The relationship between relative wave speed, damage degree and heating temperature of two types of concrete specimens after being exposed to different temperatures is shown in Figure 5. It can be seen that the relative wave speed and damage degree of concrete specimens have a good correlation with the heating temperature. As the heating temperature increases, the relative wave speed gradually decreases and the damage degree continues to increase. The reason is that the volume of the specimen expands after high temperature, the raw materials are damaged, and the specimen density decreases and the wave speed gradually decreases, which is reflected in the continuous accumulation of internal damage. An appropriate function is used for regression analysis. The fitting results are shown in Table 7. The fitting correlation coefficients are all greater than 0.95. The experimental values and the fitted values are in good agreement, indicating that the relative wave speed and damage degree are used to evaluate the internal structure of the material after high temperature. The damage is reasonable and feasible.

2.4 High Temperature Compressive Strength Loss of Concrete

It can be seen from the compressive strength loss rate in Table 6 that the strength decrease trend of the two types of concrete after high temperature is the same. When the temperature is lower than 400°C, because each specimen has undergone high-temperature autoclaved curing, only crystallized water escapes inside the concrete. The pore structure did not change significantly, and CaCO₃ with higher strength was produced, which strengthened the interlocking force between the colloid and the aggregate, so the compressive strength was improved compared with that at normal temperature. The strength of NC increased by 24.5% to the maximum after treatment at 400°C. GHB/NC has the highest strength after treatment at 200°C, increasing by 20.6%.

After 400°C, the compressive strength of each specimen dropped sharply as the temperature increased. This was due to the serious coarsening of the internal pore structure of the concrete. The C-S-H gel decomposed significantly after the temperature was higher than 600°C and lost its cementing effect. The shrinkage of cement and the softening and expansion of gravel aggregate cause cracks to expand and penetrate. When the temperature is higher than 800°C, the strength loss is nearly 80%. The cement hydration products and calcareous gravel are further decomposed. The internal water vapor forms a high vapor pressure, causing the slurry to crack or even burst at high temperature. After experiencing a high temperature of 1000°C, the cement slurry becomes loose. The specimens were almost unshaped, and the two types of concrete basically lost their bearing capacity.

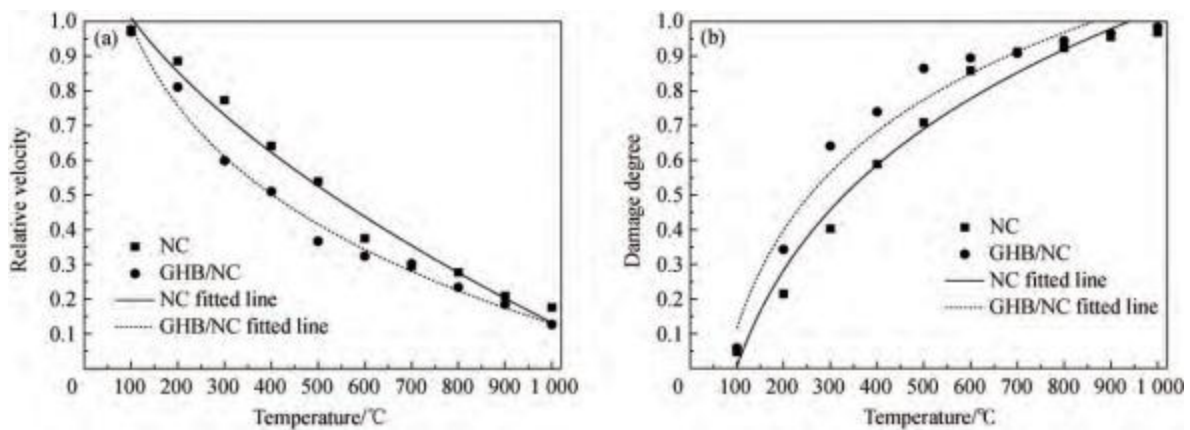


Figure 5 Relationship between ultrasonic parameters and heating temperature after high temperature for NC and GHB/NC

Table 7 Fitting results of NC and GHB/NC ultrasonic parameters and heating temperature

Concretetype	Ultrasoundparameter	Fitting formula	R2
NC	Relativevelocity vR	$vR = -22.15 \frac{T^{0.51}}{1000} + 1.33$	0.98
	Damage degree D	$D = 1.64T^{0.129} - 2.97$	0.97
GHB/NC	Relativevelocity vR	$vR = -1397.62 \frac{T^{0.1}}{1000} + 3.51$	0.99
	Damage degree D	$D = 29T^{0.006} - 63.03$	0.95

Note: T— Temperature.

2.5 Relationship Between Internal Damage and Strength Loss of Concrete

When the two types of concrete are heated from normal temperature to 1000°C, the strength undergoes a process of first slight increase and then gradual decrease. Ultrasonic wave propagation is affected by many factors and does not reflect this change pattern. Therefore, the relative wave speed, damage degree and strength are discussed. The relationship

between loss rate does not consider the influence of this temperature range for the time being. After calculation, the fitting effect is best after excluding the temperature range of 100~200°C. Figure 6 shows the experimental data and fitting effects of the relative wave speed and damage degree of the two types of concrete as they change with heating temperature. Select appropriate functions for regression analysis respectively, and the results are shown in Table 8. The fitting correlation coefficients are all greater than 0.90, and the fitting results are excellent, indicating that it is reasonable and feasible to use relative wave speed and damage degree to judge the strength loss rate.

2.6 Deterioration of Concrete Microstructural Properties

Figure 7 shows the microstructure of NC cement slurry at room temperature. It can be seen that the bonding between cement slurries is tight, complete and continuous, and there is a large amount of C—S—H gel. Acicular ettringite Aft crystals and Ca (OH) 2 can be seen under magnification. Figure 8 shows the micromorphology of NC after being heated to 200~400°C. It can be seen from Figure 8(a) that the structure of the cement hydrated slurry is basically intact after being heated to 200°C.

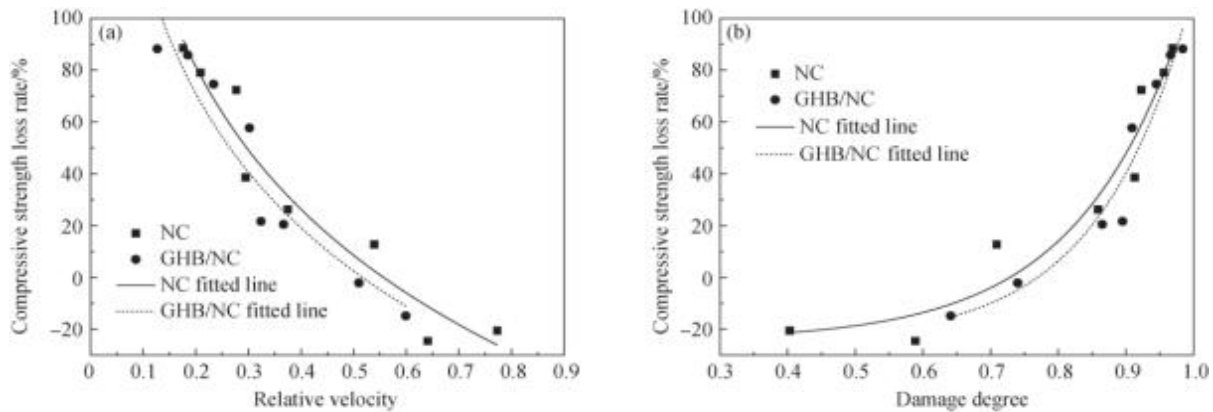


Figure 6 Relationship between ultrasonic parameters and compressive strength loss rate of NC and GHB/NC after high temperature

Table 8 Fitting results of NC and GHB/NC ultrasonic parameters and compressive strength loss rate

Concretetype	Ultrasoundparameter	Fitting formula	R2
NC	Relativevelocity vR	$\Delta F_{cu} = -79.49 \ln vR - 46.53$	0.93
	Damage degree D	$\Delta F_{cu} = 0.244e6.32D - 24.36$	0.92
GHB/NC	Relativevelocity vR	$\Delta F_{cu} = -74.74 \ln vR - 49.32$	0.88
	Damage degree D	$\Delta F_{cu} = 0.086e7.36D - 24.83$	0.92

Note: ΔF_{cu} — Compressive strength loss rate.

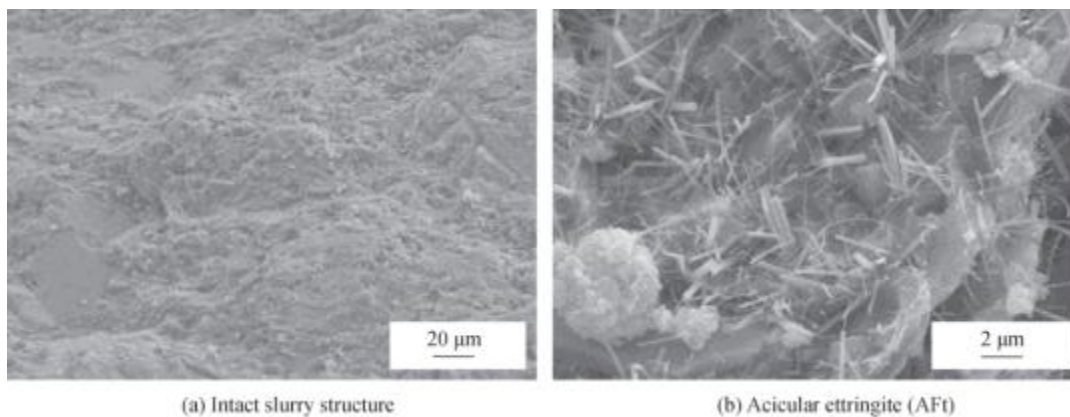
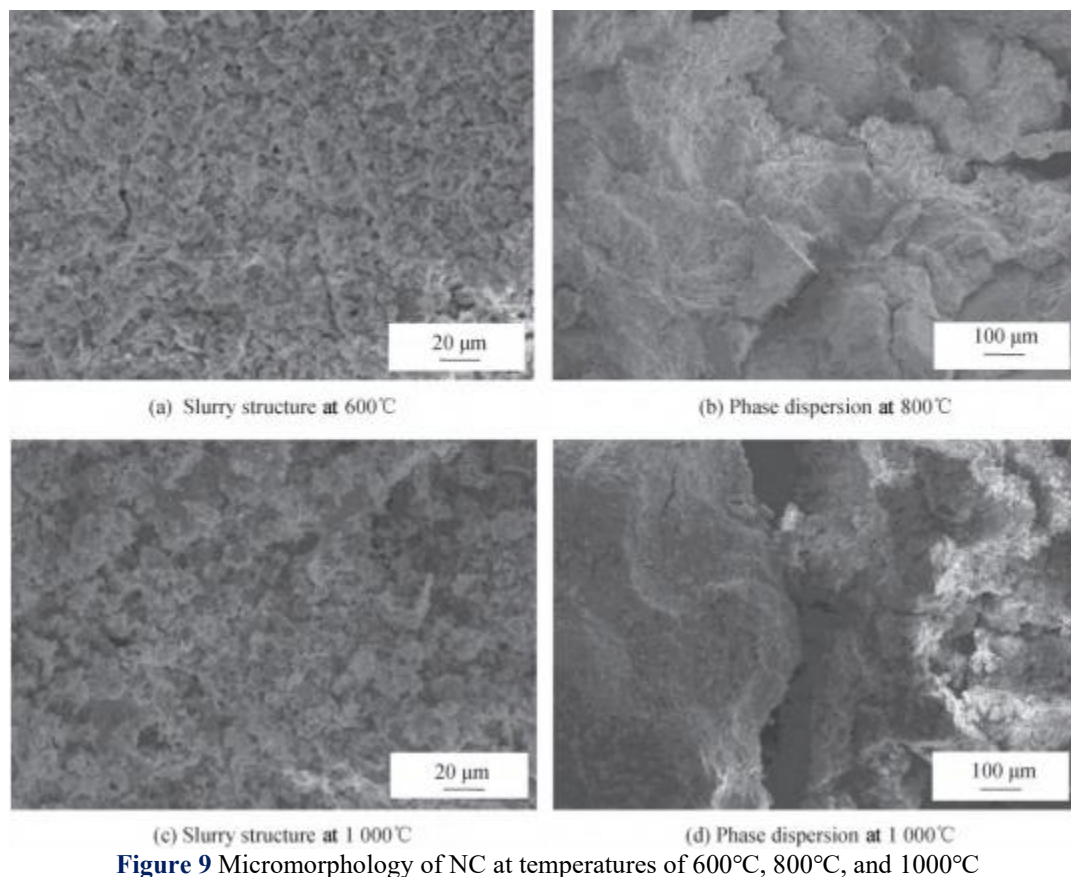
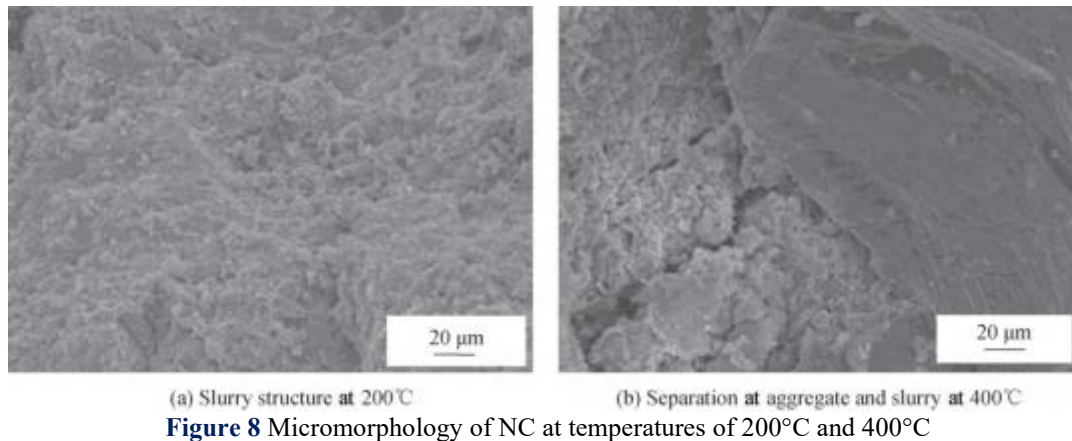


Figure 7 Microscopic morphology of NC cement slurry at room temperature

There are some signs of looseness, but all physical phases are basically normal; as shown in Figure 8(b), after being exposed to a high temperature of 400°C, the slurry becomes loose, the gel shrinks, and the aggregate and slurry separate. At this temperature range, free water, capillary water, and C-S-H gel adsorbed water are lost, promoting the cement hydration reaction and volcanic ash reaction to continue, forming a similar "autoclave curing" effect, resulting in a lower strength of the concrete specimen. The normal temperature has increased, and relevant literature also reflects this rule [21-23].

Figure 9 shows the micromorphology of NC after being heated to 600~1000°C. It can be seen from Figure 9(a) that a large amount of water is lost after 600°C, and small pores left by obvious water loss appear on the gelled surface. The cement slurry is loose, the gel decomposes, and cracks and delamination occur. The macroscopic manifestation is that the specimen whitening, cracks increased significantly; Figure 9(b) shows that the dispersion between the phases intensified after 800°C; from Figures 9(c) ~ 9(d), it can be seen that after 1000°C, the loosening of the slurry further intensified, the continuity was poor, and the dispersion between phases In severe cases, the decomposed parts have been connected into areas, cracks, and holes. On a macroscopic level, a large number of through-cracks have appeared, the volume has expanded, and the internal density and wave speed have decreased.



GHB/NC is significantly different from NC with its unique interface transition zone. Figure 10 shows the degradation process of the microstructure and morphology of the GHB/NC interface zone after high temperature treatment. It can be seen that the cement stone and vitrified microspheres are tightly combined at normal temperature, and the cement slurry enters the surface pores of the vitrified microspheres to form a tight two-phase mechanical meshing structure. The cement slurry is dense and the hydration product is in good condition; 200~400°C When the interface zone loses water, the cement slurry leaves defects such as holes after the water evaporates, but the mechanical meshing structure of the interface zone is not destroyed, and the macroscopic performance is a slight increase in strength; further heating to 600~1000°C, the cement water The slurry begins to decompose, become loose, and cracks criss-cross, producing obvious cracks and holes that penetrate each other, and the bonding force in the interface area gradually weakens.

In addition, after high temperature in the interface area between calcareous gravel and cement stone, the gravel and cement stone detach, and the interfacial bonding force is lost. It is precisely due to the combined effects of the softening and expansion of coarse aggregate as temperature increases, and the thermal decomposition and deterioration of cement hydration products that the strength of the specimen decreases significantly. After treatment at 800°C, the strength of GHB/NC was lost by 74.6%, and the strength of NC was lost. 72. 3%. After treatment at 1000°C, the strength loss of GHB/NC is 88. 2%, and the strength loss of NC is 88.5%.

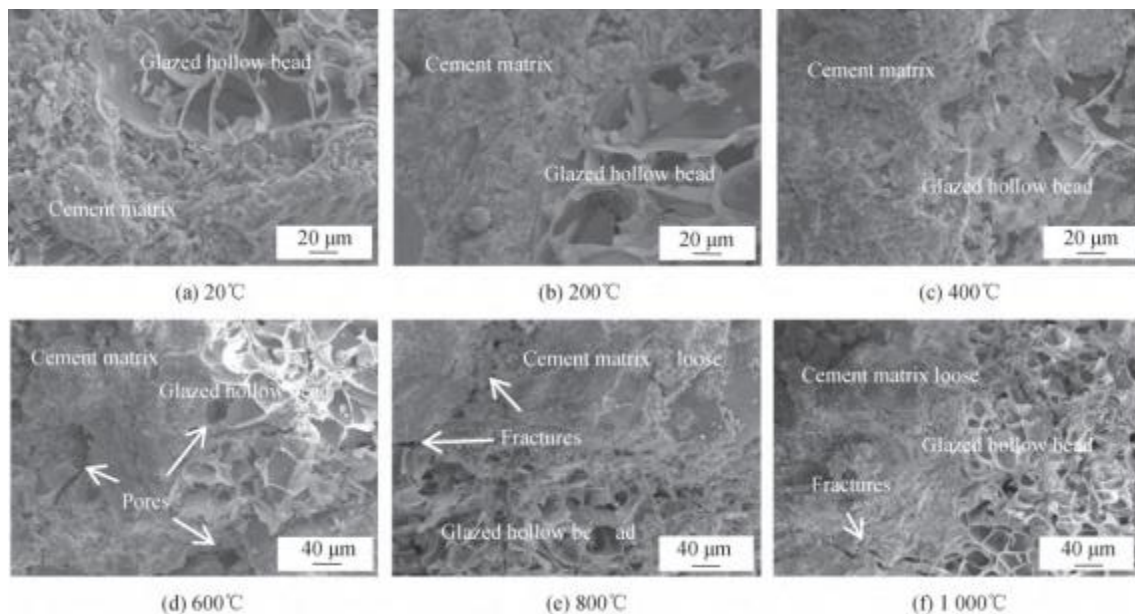


Figure 10 Microscopic morphology of the transition zone at the interface between GHB/NC vitrified microspheres and cement stone after high temperature

3 CONCLUSION

The mechanical properties, ultrasonic testing, and micromorphology of ordinary concrete (NC) and vitrified microsphere insulation concrete (GHB/NC) after high temperature were tested.

(1) Incorporating an appropriate amount of vitrified microspheres into concrete can effectively improve the heat insulation capacity of the material, the workability of the mixture, reduce the apparent density, and the compressive strength also decreases. When the heating temperature is higher than 800°C, the test block will appear to varying degrees. Damage, peeling, and peeling, the two types of concrete have similar strength loss rates after heating. After treatment at 800°C, the strength loss of NC is 72.3%, and the strength loss of GHB/NC is 74.6%. After treatment at 1000°C, the strength loss is basically lost. ability.

(2) Relative wave speed and damage degree are used to evaluate the performance deterioration of concrete after high temperature. As the heating temperature increases, the relative wave speed decreases, the damage degree gradually increases, and the compressive strength loss rate increases accordingly. The regression formula has a high fitting degree, indicating that it is reasonable and feasible to use relative wave velocity and damage degree to evaluate the degree of high-temperature deterioration of concrete.

(3) Conduct a microscopic analysis of the deterioration process of the cement slurry and the vitrified microsphere-cement stone interface transition zone after being exposed to different high temperatures. As the temperature increases, the internal cement gel gradually disperses and becomes loose from the whole, and the vitrified microspheres, coarse particles, etc. The bonding force between the aggregate and the cement stone continues to weaken and lose. The coarse aggregate softens and expands when heated, causing an increase in internal voids and surface cracks, and a loss of macroscopic strength. However, the structure of the vitrified microspheres was not significantly damaged after being exposed to a high temperature of 1000°C. It is an excellent high temperature resistant material.

COMPETING INTERESTS

The authors have no relevant financial or non-financial interests to disclose.

REFERENCES

- [1] Guo Xingzhong, Yang Chuang, Zhang Chao. Simulation study on the impact of thermal performance of energy-saving doors and windows on building energy consumption. *Journal of Building Materials*, 2014, 17(2): 261- 265, 297.
- [2] Hong Tianzhen. A close look at the China design standard for energy efficiency of public buildings. *Energy and Buildings*, 2009, 41(4): 426-435.

- [3] FANShujing, WANG Peiming. Effect of fly ashondrying shrinkage of the rmalinsulation mortar with glazed hollow beads. *Journal of Wuhan University of Technology (Materials Science Edition)*, 2017, 32(6): 1352- 1360.
- [4] Sadinenisb, Madalas, Boehm RF. Passive Building energy savings: A review of building envelope components. *Renewable and Sustainable Energy Reviews*, 2011, 15 (8): 3617-3631.
- [5] Gong Jianqing, Sun Kaiqiang. Effects of different water-cement ratios on the performance of vitrified microsphere thermal insulation mortar. *Journal of Hunan University (Natural Science Edition)*, 2017, 44(1): 143- 149.
- [6] Zhu Jiang, Li Guozhong. Performance of polypropylene fiber vitrified microsphere composite insulation materials. *Journal of Building Materials*, 2015, 18(4): 658- 662, 703.
- [7] Wu Wenjie, Yu Yiming. Study on the mix ratio of vitrified microbead thermal insulation mortar based on single factor analysis. *Materials Herald*, 2014, 28(24): 385-390.
- [8] Ma Gang, Zhang Yu, Li Zhu. Influencing factors on the interface micro hardness of lightweight concrete aggregate consisting of glazed hollow bead. *Advances in Materials Science and Engineering*, 2015, 2015: 1- 15.
- [9] Zhao Lin, Wang Wenjing, Li Zhu. An Experimental study to evaluate the effects of adding glazed hollow beads on the mechanical properties and thermal conductivity of concrete. *Materials Research Innovations*, 2015, 19(S5): 929- 935.
- [10] Zhang Yu, Ma Gang, Wang Zhangfeng. Shear behavior of reinforced glazed hollow bead insulation concrete. *Construction and Building Materials*, 2018, 174: 81-95.
- [11] Dai Xueling, Zhao Huawei, Li Zhu. Research on the application of vitrified microspheres in self-insulating walls. *Engineering Mechanics*, 2010, 27(S1): 172- 176, 183.
- [12] Gong Jianqing, Deng Guiguo, Shan Bo. Ultrasonic research and microscopic analysis of reactive powder concrete after high temperature. *Journal of Hunan University (Natural Science Edition)*, 2018, 45(1): 68-76.
- [13] Heap M J, Lavallee Y, Laumann A. The influence of thermal-stress (upto1000°C) onthe physical, mechanical, and chemical properties of siliceous-aggregate, high-strength concrete . *Construction and Building Materials*, 2013, 42: 248-265.
- [14] SHAIKH FU A., TAWHEEL M. Compressive strength and failure behaviour offibre concrete at elevated temperatures . *Advances in Concrete Construction*, 2015, 3 (4): 283-293.
- [15] Xiong Houren, Xu Jinming, Liu Yuanzhen. Experimental study on hygrothermal deformation of external thermal insulation cladding systems with glazed hollow bead. *Advances in Materials Science and Engineering*, 2016, 2016: 1- 14.
- [16] Pang Jianyong, Yao Weijing. Experimental study on new thermal insulation materials for high-temperature tunnels in deep coal mines. *Mining Research and Development*, 2016, 36(2): 76-80.
- [17] Zhao Dongfu, Liu Mei. Experimental study on residual strength and non-destructive testing of high-strength concrete after high temperature. *Journal of Building Structures*, 2015, 36(S2): 365-372.
- [18] Peng Gaifei, Yang Juan, Shi Yunxing. Experimental study on the residual mechanical properties of ultra-high performance concrete after high temperature. *Journal of Civil Engineering*, 2017, 50(4): 73-79.
- [19] Peng Gaifei, Huang Zhishan. Change in micro structure of hardened cement plaster subjected to elevated temperatures. *Construction and Building Materials*, 2008, 22(4): 593-599.
- [20] Jiang Yuchuan, Huo Da, Teng Haiwen. Research on the high temperature performance characteristics of shale ceramsite concrete. *Journal of Building Materials*, 2013, 16(5): 888-893.
- [21] Gong Jianqing, Deng Guoqi, SHAN Bo. Performance evaluation of RPC exposed to high temperature combining ultrasonic test: A case study. *Construction and Building Materials*, 2017, 157: 194-202.
- [22] Yan Lan, Xing Yongming. Effect of nano-SiO₂ on the mechanical properties and microstructure of steel fiber/concrete after high temperature. *Journal of Composite Materials*, 2013, 30(3): 133-141.
- [23] Jin Zuquan, Sun Wei, Hou Baorong. High-temperature deformation and microstructural evolution of concrete. *Journal of Southeast University (Natural Science Edition)*, 2010, 40(3): 619-623.